Optical Properties of Spherical and Oblate Spheroidal Gold Shell Colloids

J. J. Penninkhof,*,† A. Moroz,‡,|| A. van Blaaderen,*,§,⊥ and A. Polman*,†,#

Center for Nanophotonics, FOM-Institute for Atomic and Molecular Physics (AMOLF), Kruislaan 407, 1098 SJ Amsterdam, The Netherlands, Wave-scattering.com, and Soft Condensed Matter, Debye Institute, Utrecht University, P.O. Box 80000, 3508 TA Utrecht, The Netherlands

Received: November 11, 2007; In Final Form: December 27, 2007

The surface plasmon modes of spherical and oblate spheroidal core−shell colloids composed of a 312 nm diameter silica core and a 20 nm thick Au shell are investigated. Large arrays of uniaxially aligned core−shell colloids with size aspect ratios ranging from 1.0 to 1.7 are fabricated using a novel ion irradiation technique. Angle- and polarization-resolved extinction spectroscopy is performed on the arrays. Extinction spectra on spherical particles reveal dipole, quadrupole, and octupole resonances in good agreement with calculations using Mie theory. Optical extinction measurements on oblate spheroidal core−shell show strong red- and blue-shifts for polarizations along major and minor axes, respectively, that increase with size anisotropy. The measured spectral shifts of the dipole, quadrupole, and octupole resonant modes with angle and anisotropy are in good agreement with T-matrix calculations. The data provide insight into the tunable resonant behavior of surface plasmons in oblate spheroidal core−shell particles.

I. Introduction

The unusual optical properties of metal structures with dimensions smaller than or comparable to the wavelength of light are a topic of intensive research. The key concept in this field is the surface plasmon resonance, a collective resonant oscillation of the conduction electrons in the metal confined to the interface between the metal and a dielectric.

For small metal particles, the surface plasmon is confined to the particle and is therefore also called a localized surface plasmon. As is well-known, the resonance frequency strongly depends on the shape of the particle, but also on particle size and the dielectric constant of the surrounding medium.[1,2] Under illumination at resonance, the electromagnetic fields at the surface of these particles can be enhanced significantly. Because of the enhanced field intensities and the tunability of the resonances, metal nanoparticles find applications in surface-enhanced Raman scattering, fluorescence enhancement, biochemical sensing, and medical therapy and diagnostics.[3−7]

Recently, a novel class of metallo-dielectric particles, composed of a dielectric core and a metal shell, has gained strong interest.[6,8] These structures have the unique property that their surface plasmon resonance frequency is extremely sensitive to the thickness of the metal shell.[9−13] Additional tunability of the plasmon resonance can be achieved by shape anisotropy. For example, Limmer et al.[14] and Wang et al.[15] have reported on the fabrication and optical characterization of rod-like dielectric particles with a metal coating. Wang reported on a red-shift of the longitudinal plasmon resonance as the shell thickness on hematite spindles is reduced. In another recent paper,[16] egg-shaped particles were presented, with a multipeaked optical spectrum that was changing with anisotropy.

In this paper, we investigate the optical properties of spherical and oblate spheroidally shaped Au-shell particles. By using a novel method to fabricate large arrays of near-perfect ellipsoidally shaped and uniaxially aligned particles, we are able for the first time to make a direct comparison between optical extinction experiments and exact extinction calculations for these anisotropic particles.

The organization of the paper is as follows. In section II.A, the synthesis of highly monodisperse spherical Au-shell colloids is described. Sections II.B and III.C then describe the fabrication of the samples composed of oblate spheroidal particles made by MeV ion irradiation.[17] The ion beam causes an expansion of the (originally spherical) particle perpendicular to the ion beam and a contraction parallel to it. The visco-elastic nature of this process[18] leads to an oblate spheroidal shape, and the anisotropy can be accurately controlled by the ion fluence. As the ion beam direction is well-controlled, this technique enables the fabrication of ensembles of aligned monodisperse oblate spheroids that can be analyzed with far-field optical techniques. A comparison of the extinction measurements for spherical Au-shell colloids against Mie-theory calculations is presented in section III.A. In section III.B, the optical properties of oblate spheroidal Au-shell particles are investigated. Measured angle- and polarization-dependent extinction spectra are compared with T-matrix calculations. Multiple plasmon modes are observed in the spectra, and the dependence of the resonance frequencies on size anisotropy, incident angle and polarization is studied. Good agreement between experiment and theory is observed. We conclude in section IV.

II. Experimental Section

A. Synthesis of Spherical Au-Shell Colloids. Spherical Au-shell particles were fabricated using methods described in detail in ref 21 and covered with a thin silica shell as described in ref 22. The colloidal suspensions were purified by repeated

* Corresponding authors. E-mail: polman@amolf.nl; a.vanblaaderen@phys.uu.nl.
† FOM-Institute for Atomic and Molecular Physics.
‡ Wave-scattering.com.
§ Debye Institute.
|| URL: www.wave-scattering.com.
⊥ URL: www.colloid.nl.
URL: www.erbium.nl.

10.1021/jp710780j CCC: $40.75
Published on Web 02/23/2008

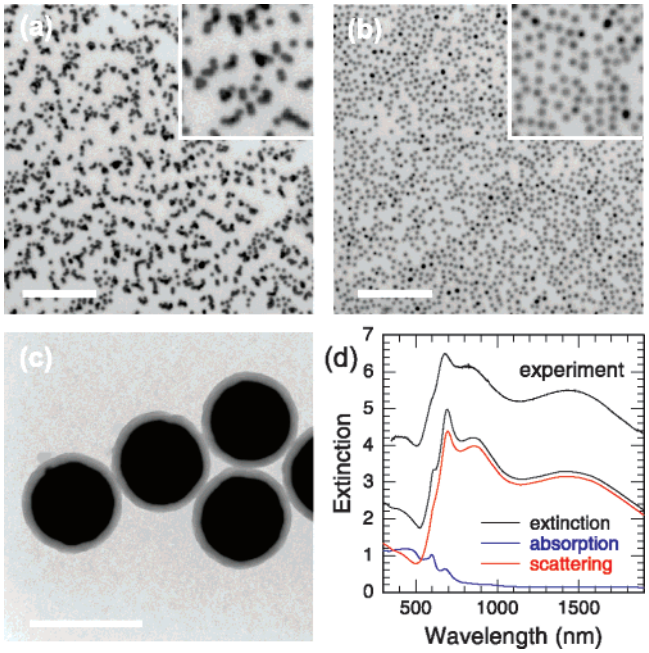

Figure 1. (a, b) Optical microscopy images taken in reflection mode of samples with Au-shell colloids at a high surface coverage, dried without (a) and with (b) use of critical point drying. The insets show an area of 9 × 9 μm^2. The scale bars in (a,b) are 10 μm. (c) Transmission electron microscopy image of particles consisting of a silica core with a radius of 156 nm, covered with a 25 nm thick Au-shell and a 40 nm thick outer silica shell. The scale bar measures 500 nm. (d) Optical extinction measurement (top) and calculation (bottom) for unirradiated spherical Au-shell particles in index matching oil (black lines). The calculated contributions of scattering (red) and absorption (blue) to the extinction are shown as well. The calculation was done for a particle with dimensions R_{core} = 156 nm and t_{Au} = 25 nm. The experimental data is scaled to the calculated data, and is offset vertically to facilitate comparison.

sedimentation and redispersion in ethanol. In this paper, we investigate particles consisting of a silica core of radius 156 nm covered with a 25-nm thick Au-shell and a 40-nm thick outer silica shell. The outer silica shell is needed during the preparation of the substrates (see section II.B) and also enhances the effect of ion irradiation.[17] The particle size was determined by transmission electron microscopy (TEM) using a Technai 12 microscope operated at 120 keV. A TEM image of these particles is shown in Figure 1c. The size polydispersity is 3% for the silica cores and about 5% for the Au-shell colloids. Assuming that the polydispersities are independent, the corresponding polydispersity in shell thickness is then 10 nm (40%).

B. Preparation of Substrates. Samples for optical measurements were made in the following way. Standard microscope slides of 1 mm or 150 μm thickness were cleaned with chromosulphuric acid and then rinsed several times with water and ethanol. The glass slides were then coated with poly(allylamine) hydrochloride (PAH, M_w = 15 000 g/mol) as described in ref 23.

Deionized water with a resistivity of 18 M Ω cm (Millipore) was further deionized by use of ion resin beads (Biorad AG 501-X8). The colloids were dispersed into the purified water to increase the thickness of the electrostatic double layer of the (negatively) charged colloids. A droplet of the suspension was then put on the (positively charged) PAH-coated substrate and the colloids were allowed to sediment for 3 h. Critical point drying with liquid CO_2 (Baltec CPD030) was used to prevent colloid clustering and/or removal by the surface tension forces that would otherwise occur during drying. This effect is clearly seen in the optical reflection microscopy images in Figure 1a,b that show two samples with the same colloid coverage dried in air (a) or with critical point drying (b). While the sample dried in air has a considerable fraction of touching particles, the sample made by use of critical point drying only contains single, nontouching particles. All samples have a coverage of less than a monolayer.

C. Ion Irradiation. MeV ion beam irradiation at 77 K was used to change the shape of the colloids from spherical to oblate spheroidal.[17] After the irradiations, the average aspect ratio (major over minor axis) of the colloids was determined by scanning electron microscopy (SEM), using a FEI XL30FEG microscope operated at 5−30 keV. Samples with colloids were irradiated by 6 MeV Au^{3+} ions at an angle of 45 ± 5° to fluences of 4 × 10^{14}, 7 × 10^{14}, and 1 × 10^{15} cm^{-2}, yielding size aspect ratios of 1.3 ± 0.15, 1.5 ± 0.2, and 1.7 ± 0.2, respectively, as deduced from SEM.

D. Optical Characterization. Optical extinction measurements were done using a dual-beam Cary 5 spectrophotometer. The samples, covered with immersion oil to match the refractive index of the substrate (Cargille Inc., Type B, Formula Code 1248, n = 1.5150), were mounted on a rotatable sample holder. The illuminated area was defined by use of circular pinholes with a diameter of 1 mm.

III. Results and Discussion

A. Extinction of Spherical Au-Shell Particles. Figure 1d shows the measured optical extinction spectrum for spherical particles embedded in immersion oil which index matches the glass (top), as well as the results of a Mie calculation of the extinction efficiency for a single particle. The extinction efficiency is defined as the extinction cross section normalized by the geometrical cross section of the particle. The experimental data were all scaled to the calculated spectra. In the calculation, the size parameters determined from TEM were taken as input parameters (R_{core} = 156 nm, t_{Au} = 25 nm). The experimental dielectric constants of Au by Johnson and Christy[24] were used to model the gold shell, with no adjustable parameters for finite-size-effects.[19,20,25] The silica core and the surrounding medium were modeled with a dielectric constant of 2.1.

In the experimental data (plotted in Figure 1d with an offset for clarity), three peaks are observed at wavelengths of about 680, 820, and 1430 nm, corresponding to the octupole, quadrupole, and dipole resonance peaks, respectively. Calculated absorption (blue) and scattering (red) spectra, also shown in Figure 1d, show that the extinction for particles of this size is mainly caused by scattering rather than by absorption. The main features in the experiment are quite well reproduced in the calculation. The slight discrepancy between experimental and theoretical spectra is attributed to the fact that the measurement was done on an ensemble of particles, whereas the calculation does not include size polydispersity. In addition, small variations in the optical constants for gold can result in significant peak shifts in the calculations. For example, for a Au-shell particle in silica with a core radius of 156 nm and a Au-shell of 25 nm, the quadrupole extinction peak wavelength varies by 15 nm using either (smoothed) data of Palik[26] or those of Johnson and Christy.[24]

Figure 2 shows calculations of the effect of shell thickness and particle size on the extinction spectra. In Figure 2a, extinction spectra are shown for particles with a core radius of 156 nm and shell thicknesses ranging from 20 to 35 nm, i.e., feasible shell thicknesses for fabrication of smooth metal shells. The contributions of the individual dipole, quadrupole, and

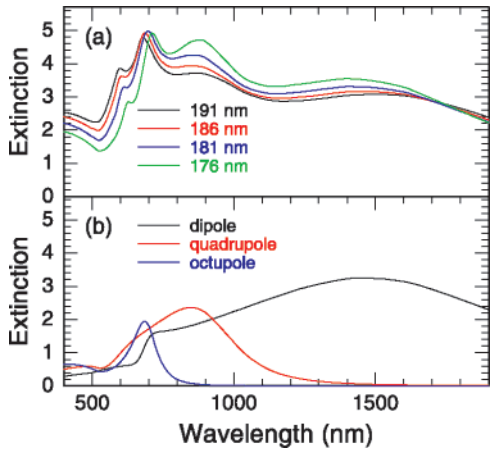

Figure 2. (a) Calculated extinction spectra for spherical Au-shell colloids with a core radius of 156 nm and shell thickness of 20 (green), 25 (blue), 30 (red), and 35 nm (black lines). (b) The individual contributions to the extinction spectrum of the dipole (black), quadrupole (red) and octupole (blue lines) modes of a Au-shell particle in silica (R_{core} = 156 nm, R_{total} = 181 nm). The experimental dielectric constants of Au by Johnson and Christy[24] were used to model the gold shell.

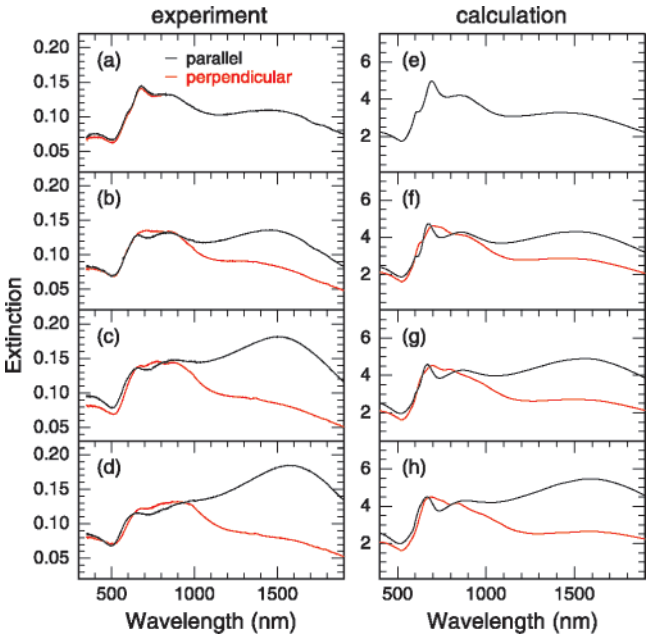

Figure 3. Measured and calculated optical extinction spectra for unpolarized light of spherical (a,e) and oblate spheroidal (b−d,f−h) Au-shell particles measured at an incidence angle of −45° (black lines) and +45° (red lines) to the sample normal, i.e., light incident approximately parallel or perpendicular to the spheroid minor axis. Size aspect ratios are 1.0 (a,e), 1.3 (b,f), 1.5 (c,g), and 1.7 (d,h).

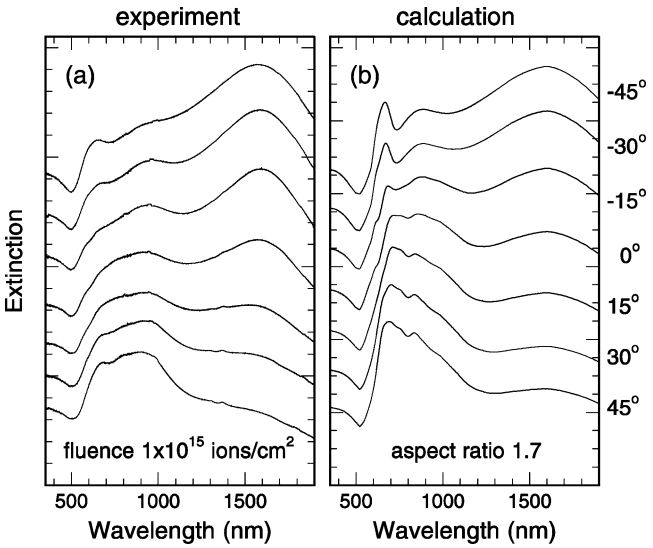

Figure 4. Optical extinction measurements (a) and calculations (b) for oblate spheroidal Au-shell particles with an aspect ratio of 1.7 at incidence angles ranging from −45° (top) to +45° (bottom) in steps of 15° (unpolarized light). Spectra are shifted vertically to facilitate comparison.

octupole modes to the overall extinction spectrum are shown in Figure 2b for a core−shell particle with core radius of 156 nm and total radius of 181 nm. Several changes are observed in the spectra of Figure 2a as the shell thickness is varied, with the largest changes seen for the quadrupole peak which almost vanishes for increasing shell thickness. By comparison of the calculated spectra and the measured spectra [Figure 1d] we deduce that the shell thickness of the colloids is in the range of 25−30 nm, in agreement with TEM data.

B. Oblate Spheroidal Au-Shell Particles. *1. Angle-Dependent Extinction Measurements.* Angle-dependent extinction spectra on arrays of aligned spheroidal core−shell particles fabricated as described in section II are shown in Figures 3−5. The spectra were measured using a rotating sample holder and obtained under both polarized and unpolarized illumination. The measurements were done at incidence angles of −45° (i.e., light approximately along the spheroid minor axis) and +45° (along the spheroid major axis), corresponding to −29° to +29° inside the sample (n = 1.5150). As a reference, the spectra of spherical colloids were also measured at these two angles [Figure 3a]; no noticeable difference is observed, as expected.

Figure 3b−d shows the extinction spectra for oblate spheroidal core−shell particles with aspect ratios of 1.3 ± 0.15 (b), 1.5 ± 0.2 (c), and 1.7 ± 0.2 (d). A clear difference is observed for the two orientations, even for the smallest size aspect ratio of 1.3. For light incident at −45° (incidence parallel to the minor axis, in black), we observe that the extinction in the infrared part of the spectrum (dipole mode) is enhanced. As the particle anisotropy is increased, the dipole mode around 1500 nm shows a gradual red-shift, while the octupole mode around 600 nm shows a slight gradual blue-shift. Illumination with light incident along the minor axis of the particles thus excites the longitudinal plasmon mode (polarization along the major axes). In the spectra for light incident at +45° (incidence perpendicular to the minor axis, in red), a broad extinction peak is observed at the positions of the quadrupole and octupole peaks, around 700 nm. In this case, for unpolarized light, both the transverse and longitudinal modes are excited.

Extinction spectra were collected over a range of angles for the silica-core/Au-shell colloids with the highest aspect ratio (fluence 1 × 10^{15} cm^{-2}, aspect ratio 1.7). In steps of 15°, the angle of the incident light with respect to the surface normal was varied from −45° to +45°. In Figure 4a, the spectra are plotted with a vertical offset for clarity. As the angle is changed from −45° (top, parallel) to +45° (bottom, perpendicular), we observe a gradual change in the shape of the spectra: the extinction in the infrared part (dipole mode region) decreases, and the extinction at 500−1000 nm (higher order modes) becomes one distinct, but broad peak.

Finally, extinction spectra were also measured under polarized light illumination (Figure 5). Spectra are shown for particles with an aspect ratio of 1.7 (fluence 1 × 10^{15} cm^{-2}), for two

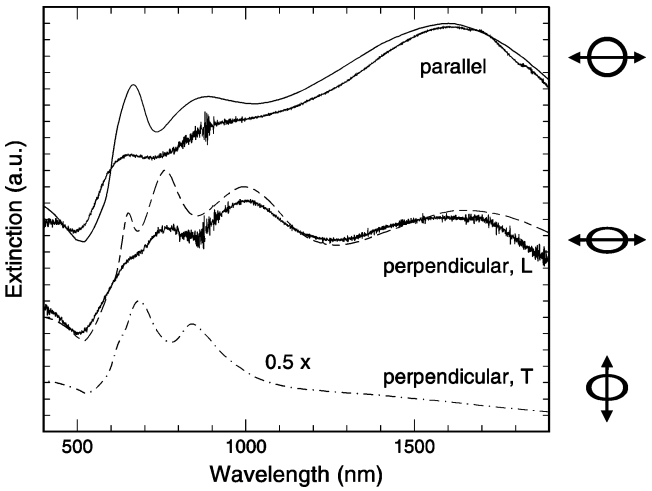

Figure 5. Measured and calculated optical extinction spectra of oblate spheroidal Au-shell particles with aspect ratio of 1.7 measured using light polarized along the major axis of the particles. Light is incident parallel (top) and perpendicular (center) to the minor axis. The top graph is shifted vertically for clarity. The spectrum for light perpendicular to the minor axis with the polarization along the short axis is also shown (dash-dotted line, vertical scale divided by 2).

orthogonal directions, parallel and perpendicular to the minor axis, with in both cases the polarization parallel to the major axis.

2. Calculations and Discussion. Calculations of the optical extinction for an oblate spheroidal silica-core/Au-shell particle in silica are shown in Figures 3−5. They were performed using the T-matrix method[27−30] with a recent improvement.[31] This method enables the calculation of extinction spectra for spheroidal core−shell particles with large permittivity. As a starting point, a spherical particle with a silica core with radius of 156 nm covered by a 25-nm thick Au-shell was used. Then, the shape of the particle was changed into an oblate spheroid, keeping the volume constant (as in the experiment). The core and the shell are considered as two concentric spheroids with identical aspect ratio, in which case the metal shell thickness is not constant over the particle. Such a shape is predicted by the viscoelastic model that describes the ion beam deformation technique that was used to prepare the aligned particles.[18,32]

Figure 3 shows the calculated extinction spectra for light incident parallel (in black) or perpendicular (in red) to the minor axis, for aspect ratios similar to the experimental values: 1 (e, sphere), 1.3 (f), 1.5 (g), and 1.7 (h). The calculated spectra clearly resemble many of the features observed in the experiments [Figure 3a−d], both for the orientations parallel and perpendicular to the symmetry axis of the particles. This provides further evidence that the anisotropic particles are well-aligned, nontouching, and relatively monodisperse. The fact that the higher-order mode peaks around 700 nm for the parallel orientation are not exactly reproduced in the experiment is attributed to the remaining particle size dispersion, mostly due to variations in the metal shell thickness (see section 2.1). The calculations also show that for unpolarized light incident perpendicular to the symmetry axis, in contrast to the orientation parallel to the symmetry axis, the peak around 700 nm is broad and without much structure, as is observed experimentally. Indeed, this direction probes a mixture of transverse and longitudinal modes, leading to a less structured resonance spectrum as will be discussed further on.

Qualitatively, the difference in extinction spectra for the different incidence angles for a spheroidal particle follows directly from a *quasistatic* approximation. For a homogeneous metallic particle the dipolar resonance wavelength is determined by the equation

$$\epsilon_m(\omega) = -\left(\frac{1}{L} - 1\right)\epsilon_b = -A\epsilon_b \quad (1)$$

where ϵ_m and ϵ_b are the permittivities of metal and surrounding medium, respectively, and L is a geometrical factor.[2] For spheroids, for polarization along the long axis $L_+ < 1/3$ and $A > 2$, while for polarization along the short axis $L_- > 1/3$ and $A < 2$. Note that for spheres $L = 1/3$, and eq 1 converges to

$$\epsilon_m \rightarrow -2\epsilon_b \quad (2)$$

Consequently, for polarization along the major axis, the resonance is red-shifted with respect to the resonance for the homogeneous particle, while the resonance for polarization along the minor axis is blue-shifted. We expect these quasistatic arguments for homogeneous metallic particles to apply, at least qualitatively, to core−shell particles as well. Indeed, these features are clearly observed in the experimental spectra of Figures 3 and 4.

In the geometry for the experiments in Figure 3, the respective L_+ and L_- resonance features can be accessed under appropriate light incidences even using unpolarized light, in line with the quasistatic arguments. For incidence parallel to the minor axis, the electric field intensity vector is always directed along a major axis and the extinction spectrum is entirely governed by the L_+ resonance. For light incident perpendicular to the minor axis, the electric field intensity vector can be decomposed into two perpendicular components one of which excites the L_- resonance, whereas the other excites the L_+ resonance. Consequently, the extinction spectrum for parallel incidence obtained using unpolarized light is determined by linear combination of the L_+ and L_- extinction spectra. Indeed, the red-shifted dipolar features observed for increasing aspect ratio in Figure 3 for incidence parallel to the minor axis are also observed (but at half the intensity) in the spectra for perpendicular incidence. Similarly, the calculated data in Figure 4 for fixed aspect ratio and varying incidence angle are composed of the appropriately weighted averages of the L_+ and L_- contributions and are in fair agreement with the data.

The respective L_+ and L_- features can be unambiguously resolved under polarized light illumination. Figure 5 shows the measured polarized extinction spectra for particles with an aspect ratio of 1.7 together with the calculated extinction spectra. The top and middle spectra are both taken with polarization along a major axis, for two incident directions (parallel and perpendicular to the minor axis). Clear differences are observed between the spectra, in both experiment and calculation. The T-matrix calculations match the experimental dipole peak around 1600 nm rather well and show a higher-order multipole structure between 600 and 1000 nm for the two incident directions, corresponding to the quadrupole and octupole modes. These calculated features are not fully resolved in the experiment, possibly due to size polydispersity as discussed above. Figure 5 also shows the calculated extinction spectrum for light incident perpendicular to the minor axis, polarized along the minor axis, a direction that was not accessible experimentally.

The unpolarized spectrum in Figure 3d for light incident perpendicular to the minor axis can be fully reconstructed from the polarized spectra of Figure 5. Indeed, T-matrix calculations show that polarization cross-terms are negligible for this case, so that the unpolarized spectrum can be derived from the average of the two polarized spectra. The result corresponds well to the

broad and unstructured peak in the spectrum observed for unpolarized light in Figure 3d.

IV. Conclusions

In conclusion, we have investigated the optical properties of spherical and oblate spheroidal Au-shell colloids in a size range beyond the quasistatic limit. Polarization and angle-dependent extinction spectroscopy is performed on uniaxially aligned arrays of particles with size aspect ratios in the range of 1.0−1.7. Measurements of the dipole, quadrupole, and octupole resonances on spherical core−shell particles show good agreement with calculations using Mie theory. For thin metal shells (15−20 nm), the resonances show a blue-shift with increasing shell thickness, in qualitative agreement with quasistatic arguments. Angle- and polarization-dependent extinction measurements on spherical and oblate spheroidal core−shell particles are in good agreement with T-matrix calculations. Strong red- and blue-shifts of the resonance spectra are observed for increasing size anisotropy. Extinction spectra for different polarizations taken along the spheroids minor and major axes are in good agreement with calculations. The data provide a comprehensive insight in the tunable resonant behavior of plasmon resonances in oblate spheroidal particles.

Acknowledgment. C. M. Graf (University of Berlin) is gratefully acknowledged for her help with the synthesis of the Au-shell particles and the initial transmission measurements. The authors acknowledge J. H. J. Thijssen and A. Imhof (Utrecht University) and S. Bidault (FOM-AMOLF) for stimulating discussions. L. W. Jenneskens and C. van Walree (Utrecht University) are thanked for the use of the CARY 5 spectrophotometer. This work is part of the research program of the "Stichting voor Fundamenteel Onderzoek der Materie (FOM)", which is financially supported by the "Nederlandse organisatie voor Wetenschappelijk Onderzoek (NWO)".

References and Notes

(1) Kreibig, U.; Vollmer, M. *Optical properties of metal clusters*; Springer: Berlin, 1995.

(2) Bohren, C. F.; Huffman, D. R. *Absorption and scattering of light by small particles*; Wiley: New York, 1983.

(3) Maier, S. A.; Atwater, H. A. *J. Appl. Phys.* **2005**, *98*, 011101.

(4) McFarland, A. D.; Van Duyne, R. P. *Nano Lett.* **2003**, *3*, 1057.

(5) Haes, A. J.; Zou, S. L.; Schatz, G. C.; van Duyne, R. P. *J. Phys. Chem. B* **2004**, *108*, 109.

(6) Hirsch, L. R.; Gobin, A. M.; Lowery, A. R.; Tam, F.; Drezek, R. A.; Halas, N. J.; West, J. L. *Ann. Biomed. Eng.* **2006**, *34*, 15.

(7) Tovmachenko, O. G.; Graf, C.; van den Heuvel, D. J.; van Blaaderen, A.; Gerrisen, H. C. *Adv. Mater.* **2006**, *18*, 91.

(8) Halas, N. J. *MRS Bull.* **2005**, *30*, 362.

(9) Neeves, A. E.; Birnboim, M. H. *J. Opt. Soc. Am. B* **1989**, *6*, 787.

(10) Oldenburg, S. J.; Averitt, R. D.; Westcott, S. L.; Halas, N. J. *Chem. Phys. Lett.* **1998**, *288*, 243.

(11) Prodan, E.; Radloff, C.; Halas, N. J.; Nordlander, P. *Science* **2003**, *302*, 419.

(12) Prodan, E.; Nordlander, P. *J. Chem. Phys.* **2004**, *120*, 5444.

(13) Brandl, D. W.; Nordlander, P. *J. Chem. Phys.* **2007**, *126*, 144708.

(14) Limmer, S. J.; Chou, T. P.; Cao, G. *J. Phys. Chem. B* **2003**, *107*, 13313.

(15) Wang, H.; Brandl, D. W.; Le, F.; Nordlander, P.; Halas, N. J. *Nano Lett.* **2006a**, *6*, 827.

(16) Wang, H.; Wu, Y.; Lassiter, B.; Nehl, C. L.; Hafner, J. H.; Nordlander, P.; Halas, N. J. *Proc. Natl. Acad. Sci.* **2006b**, *103*, 10856.

(17) Penninkhof, J. J.; Graf, C.; van Dillen, T.; Vredenberg, A. M.; van Blaaderen, A.; Polman, A. *Adv. Mater.* **2005**, *17*, 1484.

(18) van Dillen, T.; Polman, A.; Onck, P. R.; van der Giessen, E. *Phys. Rev. B* **2005**, *71*, 024103.

(19) Klar, T.; Perner, M.; Grosse, S.; von Plessen, G.; Spirkl, W.; Feldmann, J. *Phys. Rev. Lett.* **1998**, *80*, 4249.

(20) Sönnichsen, C.; Franzl, T.; Wilk, T.; von Plessen, G.; Feldmann, J.; Wilson, O.; Mulvaney, P. *Phys. Rev. Lett.* **2002**, *88*, 077402.

(21) Graf, C.; van Blaaderen, A. *Langmuir* **2002**, *18*, 524.

(22) Graf, C.; Vossen, D. L. J.; Imhof, A.; van Blaaderen, A. *Langmuir* **2003**, *19*, 6693.

(23) Decher, G. *Science* **1997**, *277*, 1232.

(24) Johnson, P. B.; Christy, R. W. *Phys. Rev. B* **1972**, *6*, 4370.

(25) Nehl, C. L.; Grady, N. K.; Goodrich, G. P.; Tam, F.; Halas, N. J.; Haffner, J. H. *Nano Lett.* **2004**, *4*, 2355.

(26) Palik, E. D. *Handbook of optical constants of solids*; Academic Press: New York, 1985.

(27) Waterman, P. C. *Phys. Rev. D* **1971**, *3*, 825.

(28) Mishchenko, M. I.; Travis, L. D.; Lacis, A. A. *Scattering, absorption, and emission of light by small particles*; Cambridge University Press: Cambridge, 2002.

(29) Quirantes, A. *J. Quant. Spectrosc. Radiat. Transfer* **1999**, *63*, 263.

(30) Quirantes, A. *J. Quant. Spectrosc. Radiat. Transfer* **2005**, *92*, 373.

(31) Moroz, A. *Appl. Opt.* **2005**, *44*, 3604.

(32) Klaumünzer, S. *Nucl. Instr. Meth. B* **2004**, *215*, 345.